RESEARCH ARTICLE SUMMARY

ADAPTATION

Rapid adaptation and extinction in synchronized outdoor evolution experiments of *Arabidopsis*

Xing Wu†, Tatiana Bellagio†, Yunru Peng†, Lucas Czech†, Meixi Lin† *et al.*

Full article and list of author affiliations:
https://doi.org/10.1126/science.adz0777

INTRODUCTION: Contemporary evolution in natural environments is being documented in many plant and animal species. However, an integrative understanding of the dynamics of rapid adaptation to different climates—the tempo, genetic architecture, predictability, and population feedbacks—remains unclear for most species. The gold standard to experimentally study the dynamics of evolution has been represented by microbial long-term laboratory experiments combined with genome resequencing, but such experiments remain challenging in multicellular macroorganisms, especially in ecologically realistic environments.

RATIONALE: We studied the evolutionary and population dynamics of rapid adaptation in different climates with an internationally synchronized outdoor evolution experiment using the annual plant *Arabidopsis thaliana*. After coordinated planting of an equal mixture of 231 *A. thaliana* accessions, 12 replicates were established at 30 sites across Western Europe, the Mediterranean and Levant, and the United States for up to 5 years. Experimental sites spanned contrasting climates—from urban European environments to the likely edge of the species' niche, the Negev desert. Combining high-coverage sequencing of 231 founder accessions with pooled whole-genome sequencing of more than 2500 samples of surviving adults comprising more than 70,000 tissue samples in the first 3 years, we characterized the dynamics of evolution in real time across climates.

RESULTS: Standing genetic variants changed in frequency rapidly across experiments, with repeatable trends among populations within similar climates but diverging trends across contrasting climates. Allele frequency shifts significantly exceeded neutral expectations. We reason that much of such shifts may be attributed to environmental natural selection, as we observed significantly synchronized (both increasing and decreasing) trends in allele frequency shifts across independent population replicates, both within one garden and in different gardens with similar climates. Such repeatability was observed in 24 of 30 gardens. Accessions from climatically matching origins increased in frequency, following patterns of past local adaptation with the strongest signals for annual mean temperature. Yet for accessions from warm regions, where we found strong local adaptation signals, we detected evidence for a recent adaptation lag; that is, they had the highest fitness when transplanted to gardens ~1.5°C colder than their home sites.

Experimental evolution genome-environment associations (eGEA) identified genomic regions that overly diverge across climates, including both known adaptive loci, such as a florigen-encoding gene, as well as genes potentially involved in thermal response, such as *CAM5*. This gene, found in a region with low linkage disequilibrium, represented one of the most pronounced allele frequency shifts, which is best explained by selection coefficients reaching −46 to +60% from cold to warm gardens, respectively. The overall genetic architecture was highly polygenic, but allele trajectories were partially predictable using genomic offset models.

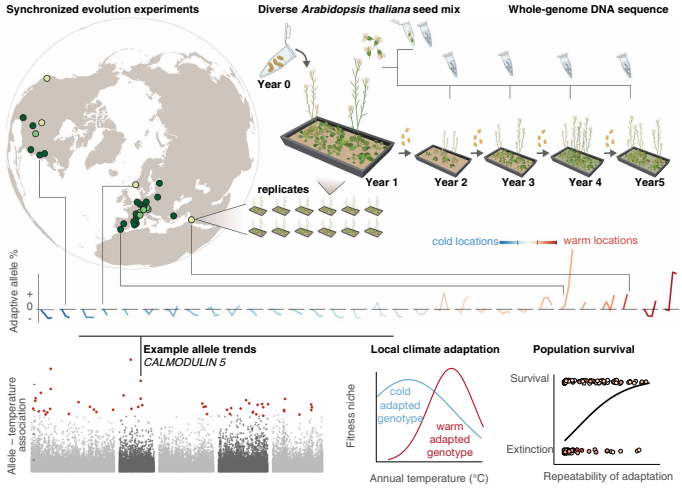

Rapid evolutionary adaptation across climates in *A. thaliana*. (Top left) A coordinated distributed evolution experiment establishing outdoor gardens with a mix of *A. thaliana* natural populations. (Top right) Populations were seeded outdoors with an equal genotype mixture, exposed to natural local climatic conditions, and whole-genome sequenced over years. (Middle center) Example allele with divergent trend along an annual temperature gradient. (Bottom left) Genome scan pointing to an example allele. (Bottom center) Estimated environment niche of the original source population either carrying or not carrying an adaptive allele. (Bottom right) Survival of replicated experimental populations after years, explained by early repeatable evolutionary trends in warm locations.

CONCLUSION: Despite evidence for rapid evolution across several climates, evolutionary trends were unpredictable in a fraction of gardens and experimental replicates. In the warmest environments, which are expected to become more prevalent with global climate change, we found that early-generation evolutionary repeatability separated persisting experimental populations from those that suffered extinction, suggesting eco-evolutionary tipping points where extreme selection overwhelms adaptive potential. Although rapid climate adaptation is possible through standing genetic variation, understanding which environmental, genetic, or species-specific conditions dictate evolutionary limits will be critical for predicting biodiversity responses to climate change. □

Corresponding author: Moises Exposito-Alonso (moisesexpositoalonso@gmail.com)
†These authors contributed equally to this work. **Cite this article as X. Wu *et al.*, *Science* 391, eadz0777 (2026). DOI: 10.1126/science.adz0777**

ADAPTATION

Rapid adaptation and extinction in synchronized outdoor evolution experiments of *Arabidopsis*

Xing Wu[1,2,3]†, Tatiana Bellagio[1,2,3,4]†, Yunru Peng[3]††, Lucas Czech[3]†§, Meixi Lin[1,2,3]†, Patricia Lang[4]¶, Ruth Epstein[1,2], Mohamed Abdelaziz[5]#, Jake Alexander[6]#, Carlos Alonso-Blanco[7]#, Heidi Lie Andersen[8]#, Modesto Berbel[5]#, Joy Bergelson[9]#, Oliver Bossdorf[10]#, Liana Burghardt[11]#, Mireille Caton-Darby[12]#, Robert Colautti[13]#, Carolin Delker[14]#, Panayiotis G. Dimitrakopoulos[15]#, Kathleen Donohue[16]#, Walter Durka[17,18]#, Gema Escribano-Avila[19]#, Steven J. Franks[20]#, Felix B. Fritschi[21]#, Alexandros Galanidis[15]#, Alfredo Garcia-Fernández[22]#, Ana García-Muñoz[22,5]#, Elena Hamann[20,23]#, Allison Hutt[24]#, José M. Iriondo[22]#, Thomas E. Juenger[24]#, Stephen R. Keller[25]#, Karin Koehl[26]#, Arthur Korte[27]#, Pamela Korte[27]#, Alexander Kutschera[28]#, Carlos Lara-Romero[22]#, Laura Leventhal[1,3,4,12]#, Daniel Maag[27]#, Arnald Marcer[29]#, Martí March-Salas[22,30]#, Juliette de Meaux[31]#, Belén Méndez-Vigo[7]#, Javier Morente-López[22,30]#, Timothy C. Morton[32]#, Zuzana Münzbergova[33,34]#, Anne Muola[35]#, Hanna Akiko Nomoto[6]#, Meelis Pärtel[36]#, F. Xavier Picó[37]#, Brandie Quarles-Chidyagwai[16,38]#, Marcel Quint[14,18]#, Niklas Reichelt[27]#, Agnieszka Rudak[39]#, Johanna Schmitt[40]#, Gregor Schmitz[31]#, Merav Seifan[41]#, Basten L. Snoek[42]#, Remco Stam[28,43]#, Marc Stift[44]#, John R. Stinchcombe[45]#, Mark A. Taylor[12]#, Peter Tiffin[46]#, Irène Till-Bottraud[47]#, Anna Traveset[48]#, Jean-Gabriel Valay[49]#, Martijn Van Zanten[50]#, Vigdis Vandvik[51]#, Cyrille Violle[52]#, Detlef Weigel[53]#, Maciej Wódkiewicz[39]#, François Vasseur[52], J. F. Scheepens[54], Moises Exposito-Alonso[1,2,3,4,55]*

Climate change forces species to adapt rapidly to avoid extinction. To directly observe rapid adaptation and extinction, we conducted synchronized evolution experiments with *Arabidopsis thaliana* in 30 locations across Western Europe, the Mediterranean, the Levant, and North America. Whole-genome pooled sequencing of ~70,000 surviving plants revealed repeatable allele frequency shifts in similar climates but divergent shifts across contrasting ones, indicating evolutionary adaptation. We identified genetic variants linked to climate adaptation, including genes involved in processes ranging from thermal-stress sensing to spring-flowering timing. Evolutionary trends were often predictable, but variable, across environments. In warmer climates, evolutionary predictability correlated with population survival over 5 years, whereas erratic changes preceded extinction. These results show that rapid climate adaptation is possible, but understanding its limits will be crucial for biodiversity forecasting.

Rapid evolutionary adaptation at ecological timescales in the wild has been documented across eukaryotes, from field mustard (*1*), barley (*2*), and Darwin's finches (*3*) to fruit flies (*4*), stick insects (*5*), and sticklebacks (*6*). Despite increasing evidence of rapid adaptation in natural environments, the extent to which rapid adaptation can rescue vulnerable populations from climate change–driven extinction is still unknown (*7*, *8*). We still do not fully understand how fast rapid evolutionary adaptation in complex environments and organisms can be, whether it will proceed through polygenic or major-effect architectures, or whether rapid adaptation will fail under certain climates.

The gold standard to experimentally study the dynamics of evolution has been microbial long-term laboratory experiments combined with genome resequencing (*9*, *10*). In these evolution experiments, adaptation typically occurs through de novo mutations over thousands of generations. By contrast, we have limited long-term field experiments with animal and plant species. Pioneered in plants (*11*), common garden and reciprocal transplant experiments are a powerful tool to compare the fitness of multiple genotypes of a species from different locales and test adaptation to an environment and have been key tools to reveal pervasive within-species variation involved in local adaptation (*12*–*14*). However, because of their short timescale, they only teach us about a species' potential for adaptation from standing variation; they do not directly observe adaptation dynamics or population rescue as it happens. Very few examples of long-term experiments in animals and plants—such as orchard studies of fruit flies (*15*, *16*) or a long-term field trial of a domesticated plant (*2*)—have shown rapid adaptation from natural selection acting on standing preexisting genetic variation (*17*) over a few generations. However, to comprehensively address gaps in our understanding of rapid climate evolution and population responses, we need data from large-scale studies of animal or plant experimental evolution, optimally replicated across continents and over multiple years, which are presently lacking.

Here, we tracked evolution for 5 years in more than 30 locations with contrasting climates by combining common garden experiments with temporal genome resequencing in the annual plant *Arabidopsis thaliana*. We found evidence of rapid evolutionary responses across climates, identified previously unknown environmental adaptation roles of genes, and predicted short-term evolutionary trends. Despite this, evolutionary adaptation was not possible across all environments, highlighting the importance of understanding not only the potential but also the limits of evolution under the exceptional pressures raised by climate change.

A synchronized evolution experiment in *A. thaliana* across climates

To understand the genetic basis of rapid evolution across a wide range of climates, we conducted a multiyear and multilocation evolution experiment in outdoor gardens using the hermaphroditic highly selfing annual plant *A. thaliana* as a model species. We established the Genomics of rapid Evolution to Novel Environment network (GrENE-net) consortium (www.GrENE-net.org) to implement a simplified and standardized protocol for evolution experiments (see protocol in supplementary text S1). Experiments were coordinated in 43 locations across Europe, the Levant, and the United States (Fig. 1, fig. S1, and table S1) and began in the fall of 2017. Experimental sites spanned contrasting climates from urban European environments to the likely edge of the species' niche, the Negev desert. At each location, 12 independent replicate trays of plants were established and maintained for up to 5 years (*A. thaliana* typically undergoes one generation per year with a spring flowering or, in some climates, two generations with spring and fall flowering). Experimental trays were filled with homogenized soil, tagged with temperature and humidity sensors, placed outdoors to grow with minimal human intervention (i.e., no watering, fertilization, or shelter), and sown with ~15,000 seeds of the same founder genotypes: 231 *A. thaliana* accessions. These accessions were selected to represent standing genetic variation across the entire native geographic range of *A. thaliana*, mixed at roughly equal proportions, and validated by whole-genome sequencing [Fig. 1A and table S2; see sequence validation in supplementary text S4 and S5, figs. S12 and S13, and datasets S4 and S5 in (*18*)]. The population in each tray reproduced naturally, allowing for the study of demography and evolution across generations and climates. In predominantly self-fertilizing populations, adaptation is expected to advance through the differential

fitness of inbred lineages, whereas any outcrossing that does occur generates recombinant genotypes on which selection can act at a finer genomic scale. We detected signs of outcrossing in ~6 to 17% of samples (see supplementary text S10 and fig. S14), in line with observations from natural populations (*19*). Out of 43 initial sites, seven sites failed because of experimental logistics, and six sites established populations that all died off within a few months, possibly because of extreme climatic conditions. Plants from the remaining 30 sites successfully reproduced for at least one generation and yielded genomic and demographic data (table S6).

Here, we present genomic data from the first 3 years of GrENE-net (2017–2020), along with complete census and environmental data (2017–2022) [phase I data release, www.GrENE-net.org/data and (*20*)]. This includes daily climate data [dataset S2 in (*18*)], biweekly per-tray photographs from the growing seasons [dataset S3 in (*18*)], 1141 demographic measurements [fig. S5, table S3, and dataset S1 in (*18*)], and 74,491 tissue samples of reproductive plants collected and sequenced in 2415 pools (figs. S2 and S4 and table S5) (*21*). Each genomic DNA library was generated from 1 to ~200 pooled flowers collected from a single tray of surviving plants at standardized sampling times, providing a snapshot of the genetic makeup of the reproductive population (Fig. 1, A to C, and supplementary text S1 and S2). For each sample, we reconstructed allele frequencies for ~3.2 million single-nucleotide polymorphisms (SNPs) with an estimated ~0.7% error rate, with linkage disequilibrium (LD) decay in the founder population of ~7 kb (fig. S12). To achieve this, we combined allele count information from ~10× coverage depth of pool-sequencing per experimental population sample and error reduction using linkage in the 231 founder accessions from ~22× [interquartile range (IQR): 15.7 to 34.9] coverage sequencing [supplementary text S5, figs. S11 to S13, and datasets S6 and S7 in (*18*)], following established methods from the evolve and resequence literature (*22*, *23*). The composition of 231 founder accessions in the starting seed mix was also reconstructed by high coverage sequencing of the seed mix, confirming a very even representation of 0.5% per accession (i.e., 1/231) with a 0.1% error rate (supplementary text S5 and fig. S12). By merging data from multiple samplings of the same tray and growing season, we generated genome-wide allele frequencies and accession relative frequencies of 738 replicated populations across 30 locations, spanning up to 12 replicate populations per location (average ~11 populations) and up to three sequenced years (i.e., equivalent to three to six generations in addition to the starting generation). Combining these paired environmental and demographic metadata with evolutionary trajectories, we then studied the patterns and genomic architecture of rapid evolution across climates.

Evolution is rapid across climates in GrENE-net

To directly study rapid adaptation from standing genetic variation, we analyzed genome-wide allele frequency changes and population differentiation across all generations and experimental gardens. We reasoned that allele frequency trends that are significantly synchronized (increasing or decreasing) across independent population replicates within one garden (i.e., within-garden repeatability from standing variation) or different gardens of similar climate (i.e., cross-garden parallelism) must reflect the action of natural selection.

We first measured the degree of population differentiation by comparing shifts in allele frequencies between starting founder and evolved populations across time and space using the fixation index (F_{ST}) for pool sequencing (*24*). We observed that the median F_{ST} across all experimental gardens with respect to the founder population increased with each generation, indicating the gradual differentiation from the founder population over time (across all samples: $F_{ST\ y1\ median\ [IQR]} = 0.002$ [0.001–0.006], $n = 319$ populations with >1 flower samples, $F_{ST\ y2\ median\ [IQR]} = 0.017$ [0.010–0.036], $n = 217$ populations, $F_{ST\ y3\ median\ [IQR]} = 0.024$ [0.010–0.055], $n = 182$ populations; fig. S19A). In addition, F_{ST} divergence was larger between-gardens compared with within-gardens {$F_{ST\ mean\ within\text{-}garden} = 0.041$, [95% confidence interval (CI): 0.039–0.042], $F_{ST\ mean\ between\text{-}garden} = 0.052$, [95% CI: 0.051, 0.052]; fig. S19B}. To better understand population divergence across environments, we then decomposed allele frequency changes of evolved populations across all gardens using a principal components analysis (PCA) and diffusion maps (Fig. 2A and figs. S20 and S21). The major axes of allele frequency change separate evolved populations according to the climate of the experimental gardens they were planted in, where experiments in similar climates led to similar evolutionary trajectories and vice versa {mixed model regression between allelic frequency PC1-annual mean temperature (BIO1) with garden and year as hierarchical random effects, $b = 0.307$ [95% CI: 0.091–0.524], $n = 738$ populations, $n = 30$ gardens}.

To test whether the observed magnitude of evolution was significantly larger than expected from neutral genetic drift, we compared

[1]Department of Integrative Biology, University of California Berkeley, Berkeley, CA, USA. [2]Howard Hughes Medical Institute, University of California Berkeley, Berkeley, CA, USA. [3]Department of Plant Biology, Carnegie Institution for Science, Stanford, CA, USA. [4]Department of Biology, Stanford University, Stanford, CA, USA. [5]BioChange, Department of Genetics, University of Granada, Granada, Spain. [6]ETH Zürich, Institute of Integrative Biology, Zürich, Switzerland. [7]Plant Molecular Genetics Department, Centro Nacional de Biotecnología (CNB-CSIC), Madrid, Spain. [8]Department of Natural History, University of Bergen, Bergen, Norway. [9]Center for Genomics and Systems Biology, New York University, New York, NY, USA. [10]Institute of Evolution and Ecology, University of Tübingen, Tübingen, Germany. [11]Plant Science Department, The Pennsylvania State University, University Park, PA, USA. [12]Department of Evolution and Ecology, University of California Davis, Davis, CA, USA. [13]Biology Department, Queen's University, Kingston, ON, Canada. [14]Institute of Agricultural and Nutritional Sciences, Martin-Luther-University Halle-Wittenberg, Halle (Saale), Germany. [15]Biodiversity Conservation Laboratory, Department of Environment, University of the Aegean, Mytilene, Lesbos, Greece. [16]Department of Biology, Duke University, Durham, NC, USA. [17]Department of Community Ecology, Helmholtz Centre for Environmental Research-UFZ, Halle, Germany. [18]German Centre for Integrative Biodiversity Research (iDiv) Halle-Jena-Leipzig, Leipzig, Germany. [19]Proyecto Mejora Conocimiento THIC, Grupo Tragsa – SEPI, Madrid, Spain. [20]Department of Biological Sciences and the Louis Calder Center, Fordham University, Bronx, NY, USA. [21]Division of Plant Science and Technology, University of Missouri, Columbia, MO, USA. [22]Global Change Research Institute, Rey Juan Carlos University, Móstoles, Madrid, Spain. [23]Plant Ecology and Evolution, Heinrich-Heine-Universität Düsseldorf, Germany. [24]Department of Integrative Biology, University of Texas at Austin, Austin, TX, USA. [25]Department of Plant Biology, University of Vermont, Burlington, VT, USA. [26]Max Planck Institute of Molecular Plant Physiology, Potsdam-Golm, Germany. [27]Department of Pharmaceutical Biology, Julius-von-Sachs-Institute of Biosciences, Julius-Maximilians-Universität Würzburg, Würzburg, Germany. [28]Chair of Phytopathology, Technical University of Munich, Freising, Germany. [29]CREAF, Bellaterra (Cerdanyola del Vallès), Catalonia, Spain. [30]Plant Evolutionary Ecology, Faculty of Biological Sciences, Goethe University Frankfurt, Frankfurt am Main, Germany. [31]Plant Molecular Ecology, University of Cologne, Cologne, Germany. [32]Department of Ecology and Evolution, University of Chicago, Chicago, IL, USA. [33]Department of Botany, Faculty of Science, Charles University, Prague, Czech Republic. [34]Institute of Botany, Academy of Sciences of the Czech Republic, Průhonice, Czech Republic. [35]Division of Biotechnology and Plant Health, Norwegian Institute of Bioeconomy Research, Tromsø, Norway. [36]Institute of Ecology and Earth Sciences, University of Tartu, Tartu, Estonia. [37]Departamento de Ecología y Evolución, Estación Biológica de Doñana (EBD-CSIC), Sevilla, Spain. [38]Department of Plant Biology, University of California Davis, Davis, CA, USA. [39]University of Warsaw, Faculty of Biology, Warsaw, Poland. [40]Center for Population Biology, University of California Davis, Davis, CA, USA. [41]Mitrani Department of Desert Ecology, Swiss Institute for Dryland Environmental and Energy Research, Ben-Gurion University of the Negev, Beersheba, Israel. [42]Theoretical Biology and Bioinformatics, Institute of Biodynamics and Biocomplexity, Utrecht University, Utrecht, Netherlands. [43]Institute of Phytopathology, Christian-Albrechts University, Kiel, Germany. [44]Ecology, University of Konstanz, Konstanz, Germany. [45]Ecology and Evolutionary Biology, University of Toronto, Toronto, ON, Canada. [46]Department of Plant and Microbial Biology, University of Minnesota, St. Paul, MN, USA. [47]Université Clermont Auvergne, CNRS, GEOLAB, Clermont-Ferrand, France. [48]Global Change Research Group, Mediterranean Institute of Advanced Studies (IMEDEA, CSIC-UIB), Esporles, Mallorca, Balearic Islands, Spain. [49]Jardin du Lautaret, Université Grenoble Alpes, CNRS, Grenoble, France. [50]Plant Stress Resilience, Institute of Environmental Biology, Utrecht University, Utrecht, Netherlands. [51]Department of Biological Sciences, University of Bergen, Bergen, Norway. [52]CEFE, Université Montpellier, CNRS, EPHE, IRD, Montpellier, France. [53]Max Planck Institute for Biology Tübingen, Tübingen, Germany. [54]Faculty of Biological Sciences, Goethe University Frankfurt, Max-von-Laue-Str. 13, Frankfurt, Germany. [55]Innovative Genomics Institute, University of California, Berkeley, CA, USA. ***Corresponding author. Email: moisesexpositoalonso@gmail.com**
†These authors contributed equally to this work. ‡Present address: The Edison Family Center for Genome Sciences and Systems Biology, Washington University School of Medicine, St. Louis, MI, USA. §Present address: Section for GeoGenetics, Globe Institute, University of Copenhagen, København, Denmark. ¶Present address: Department of Plant and Microbial Biology, University of California Berkeley, Berkeley, CA, USA. #Genomics of rapid Evolution to Novel Environment network (GrENE-net) consortium member.

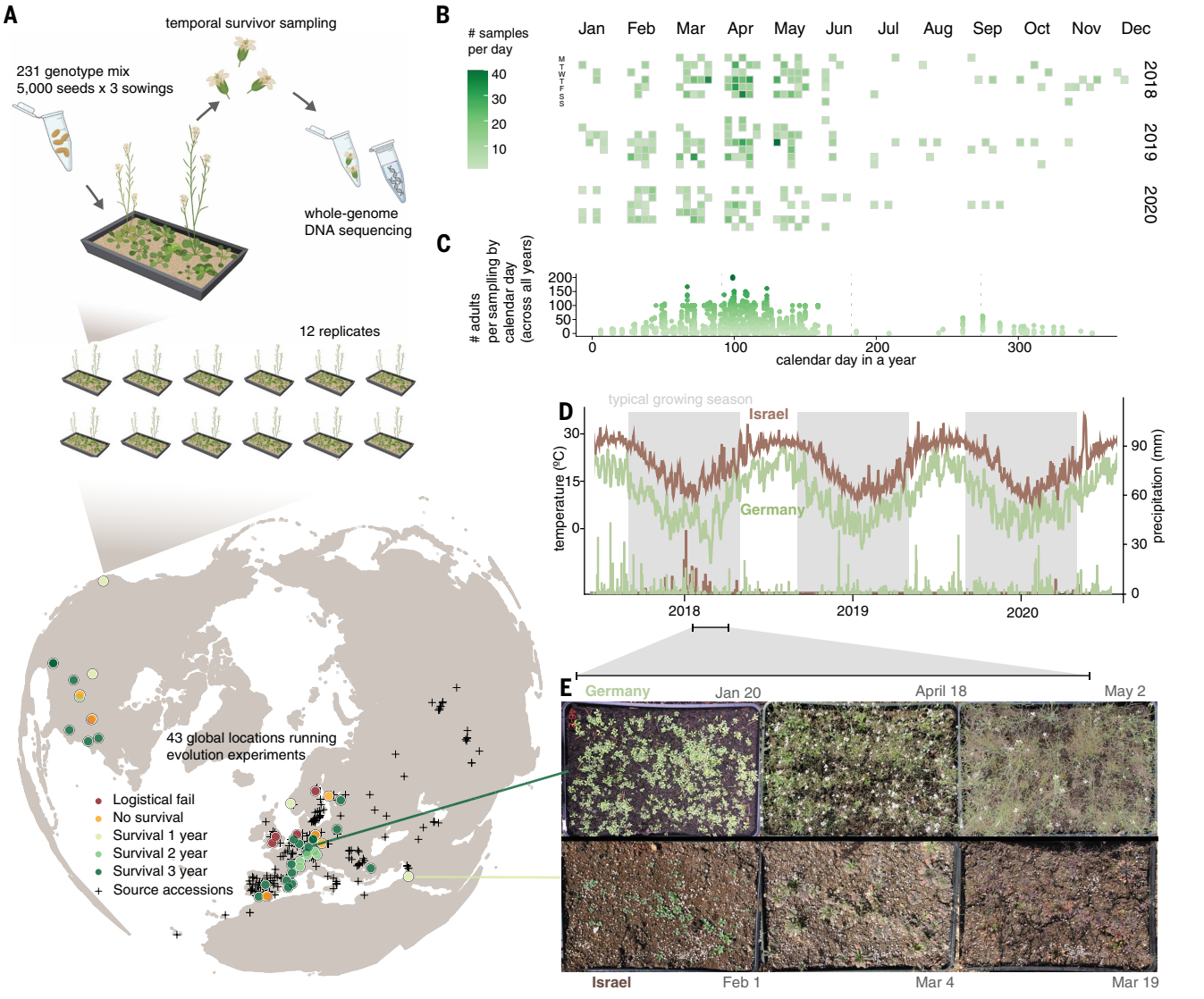

Fig. 1. GrENE-net's globally distributed evolution experiment of *A. thaliana*. (**A**) GrENE-net experimental design with 231 *A. thaliana* accessions mixed in tubes of ~5000 seeds. Each experimental tray was sown with three tubes, and seeds were sown every 2 weeks throughout fall 2017 to ensure establishment. Each site started 12 trays as independent experimental replicates. The map shows 43 gardens (sites) where participants started the experiment; colors indicate experiment outcomes, with 30 sites successfully completing at least one generation and producing genomic data. [Figure cartoons created with BioRender.com] (**B**) Calendar of time-series collections of flower tissues used for genomic sequencing for the first 3 years. (**C**) Density of samples collected along the calendar year, combining data from all 3 years. (**D**) Daily temperature curves and precipitation bars over the first 3 years of the experiment in two example locations: humid continental (Würzburg, Germany; site no. 46; green) and arid desert (Sde Boker in the Negev desert, Israel; site no. 26; brown). (**E**) Example photographs of the experimental populations in Germany and Israel during spring of the first growing season.

the observed variance of allele frequency (p) changes [$Var_{observed} = Var(\Delta p) = (p_1 - p_0)^2$) with neutral evolution expectations from theory and simulations. Our rationale is that genetic drift naturally creates shifts in allele frequencies from just stochastic sampling, which can be measured as genome-wide variance in frequency change. Then, if we find larger observed shifts than expectations from several stochastic demographic processes, we will need to invoke other evolutionary forces. First, comparing observed frequency variance in experimental populations with the classic Wright-Fisher (WF) population expectation [$Var_{WF} = p_0(1 - p_0)/2N$], we found, on average, threefold larger shifts across samples of different population sizes and starting allele frequency classes ($Var_{observed}/Var_{WF} = 2.99$ [95% CI: 2.94–3.04], assuming N as the sample size sequenced, which yields a conservative test; figs. S16 and S17 and supplementary text S7). Larger allele frequency deviations would be expected if WF assumptions were violated, such as because of a lack of complete outcrossing or equal reproduction contributions, which are common in naturally evolving *A. thaliana* populations. We then conducted another set of non-WF neutral simulations by sampling random accessions (i.e., sorting without outcrossing) and unequal Poisson reproduction, which one may expect to dominate evolutionary dynamics in highly self-fertilizing species (see supplementary text S7). We still found significantly larger observed frequency changes than expected under non-WF sorting dynamics, especially in experimental replicates of larger population sizes (fig. S17), with increasing deviations of observed evolution from neutral expectations ($t_0 \rightarrow t_1$: $Var_{observed}/Var_{neutral\text{-}sorting} = 1.379$ [IQR: 0.982–1.658], where t is the temporal sampling year; across allele frequency classes and sample sizes; Fig. 2A, figs. S15 to S17, and supplementary text S7 and S8).

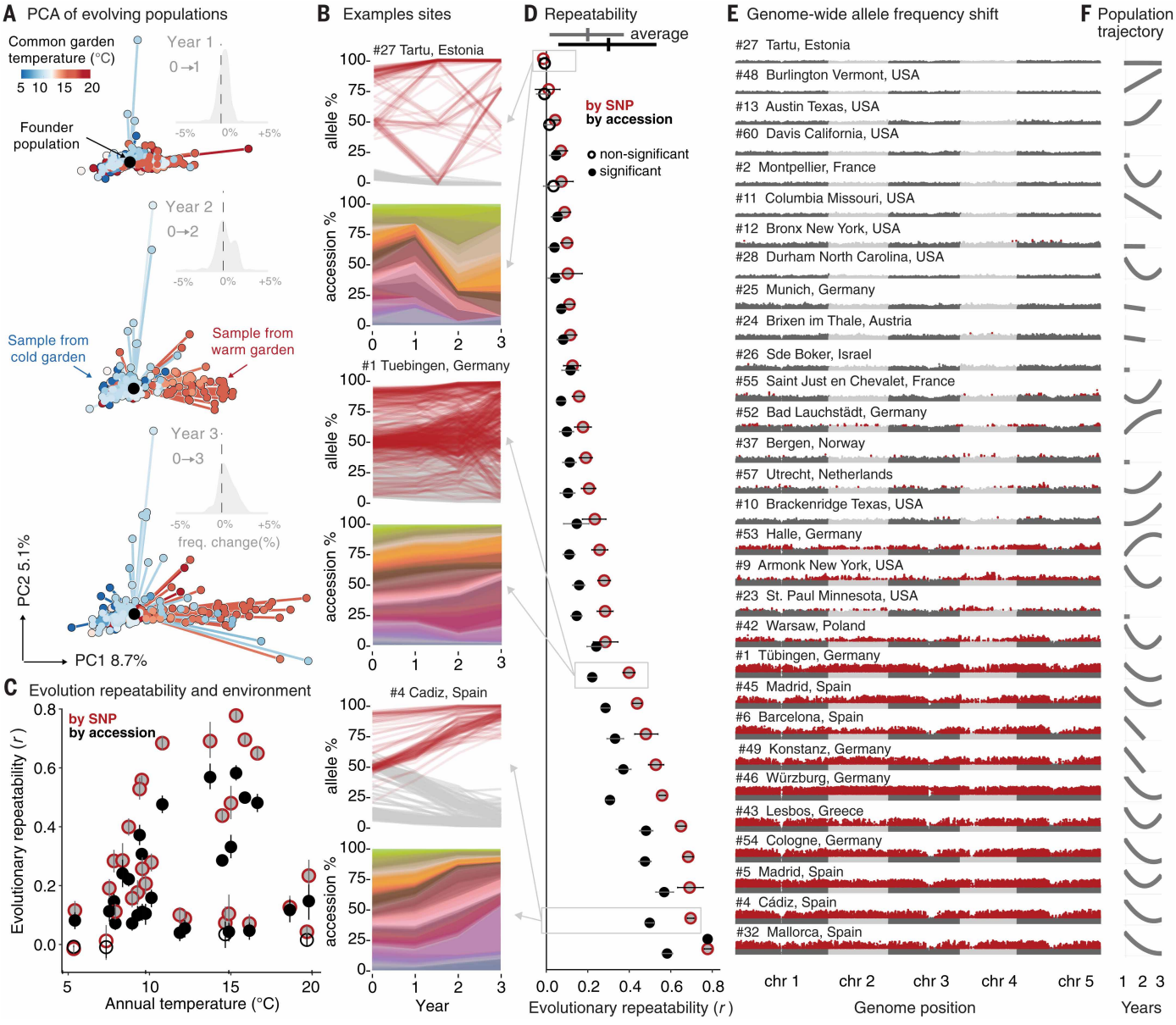

Fig. 2. Genomic evolution in GrENE-net is rapid and parallel. (**A**) PCA of allele frequencies and samples over three generations with up to 12 replicates per location ($n = 738$). The genome-sequenced founder population, common to all experiments, was projected into the PCA space (black). Insets show the distribution of genome-wide allele frequency changes between generations. (**B**) Example of three sites with low, intermediate, and high evolutionary repeatability displayed at the allele and accession level. At the allele level, the 100 fastest increasing (red) or decreasing (gray) allele frequencies over time are plotted for illustration. At the accession level, all 231 accessions are displayed using a Muller plot with accessions sorted based on the temperature of origin from colder (green to yellow) to warmer (purple to blue). (**C** and **D**) Evolutionary repeatability within-garden measured as correlation in change of frequency in the first generation (either an allele or accession relative abundance) between two pairs of population replicates within one garden. Circles indicate the mean of pairwise Pearson's correlation, and lines indicate standard error. Filled circles indicate statistically significant correlations, and open circles indicate correlations not different from zero. Within-garden repeatability is displayed against the garden annual temperature (C) or as a vertical rank (D). (**E**) Manhattan plots of genome-wide LRTs of alleles changing in frequency across 12 replicates within a site in the first generation (red indicates alleles with significant natural selection under Bonferroni correction). (**F**) Population trajectories of each location estimated across all years and replicates displaying the fitting of a polynomial regression (for expanded visualization, see fig. S9).

Having established that allele frequency changes significantly depart from several neutral stochastic expectations, we hypothesized that environment-driven natural selection may have created larger, deterministic allele trajectories. Such natural selection should create repeatable allele frequency shifts in multiple replicates in the same garden [i.e., correlation of $(p_1 - p_0)$ between replicates i and j; see supplementary text S9]. We found significant within-garden repeatability in 24 out of 30 gardens, as shown by high rank correlations of genome-wide allele frequency trends (Fig. 2, B to D, and figs. S24 to S28; mean[sd] $r_{\rho\,snp} = 0.293$ [0.237], e.g., highest repeatability within site no. 32 Mallorca, Spain, $r_{\rho\,snp} = 0.778$ [95% CI: 0.762–0.794]). Repeatable trends across replicates can be further used to map genomic regions with more predictable frequency. Using a likelihood-ratio test (LRT-1; supplementary text S11) (*25*), we found that such signals were widespread along the genome, likely owing to many alleles being linked to causal loci and thus experiencing indirect or linked selection (*26*) (Fig. 2E). Overlaying the selection signals onto 16,917 LD blocks along the *A. thaliana* genome estimated in the founder population [supplementary text S12 in (*20*)], we identified 377 LD blocks that presented signals of natural selection in 10 or more gardens (the evidence of

genomic convergence, overlap is higher than expected by permutation test, $P < 10^{-6}$; fig. S31), suggesting that adaptation through standing variation may be rapid and highly polygenic.

An additional way to evaluate selection on standing variation is by analyses of accession sorting. We reconstructed the relative abundance of the 231 founder *A. thaliana* accessions over time using allele frequencies from pool sequencing and the genomes of the founders. We note that although we detected some outcrossing (supplementary text S10 and fig. S14), ignoring outcrossing allows us to implement this intuitive analysis of accession frequency evolution. Muller plots reveal patterns akin to strain evolution in microbial studies (Fig. 2B and figs. S22 and S23) where multiple adaptive variants are competing to rise in frequency (*10*). These dynamics are expected because the starting population was rich in standing genetic variation. Following the previous rationale that deterministic trends of accession relative frequency must be at least partially due to differences in fitness of accessions, and thus natural selection, we also found high rank correlation of accessions' relative frequency, showcasing repeatable trends within garden environments (Fig. 2, B and C; mean[sd] $r_{\rho\ \text{accession}} = 0.194$ [0.179], $n = 30$ gardens). Another approach to the repeatability in frequency shifts used in evolve-and-resequence experiments has aimed to use covariances of allele frequencies to infer heritability of fitness differences among genotypes (*27*). By having accession relative frequency in multiple replicates within a garden, a proxy heritability of relative abundances of accessions can be simply estimated using random effect regression ($H^2_{\text{range}} = 12.9$ to 79.6%, $n = 30$ gardens), and indeed strongly correlates with repeatability (correlation $H^2 - r_\rho$ within-garden repeatability, $r = 0.93$, $P = 5.3 \times 10^{-14}$, $n = 30$ gardens; see supplementary text S9).

Not only did similar accessions rise in frequency in replicates within an environmental garden, but they also prospered in parallel across gardens of similar climates. For example, we see strongly parallel changes in three cold locations in Germany (mean $r_{\text{across cold gardens}} = 0.451$ [95% CI: 0.443–0.459]) and three warm locations in south Spain ($r_{\text{across warm gardens}} = 0.453$ [95% CI: 0.437–0.468]; fig. S29), indicating that similar relative fitness ranks of accessions are maintained in similar environments, even in geographically distinct locations (*28*, *29*). Correlations among replicates within gardens were naturally higher than correlations between gardens of similar climates ($r_{\text{within cold gardens}} = 0.548$ [0.534–0.562], $r_{\text{within warm gardens}} = 0.699$ [0.682–0.716]; fig. S29), which may be attributable to technical factors in the experimental design (e.g., correlated experimenter temporal sampling, or dispersal among trays, although our dispersal estimates indicate that <1% of seeds in a tray could be migrants; fig. S3). Alternatively, these results may indicate that the environmental selection pressures are complex and specific to each garden, even if we classify several gardens as belonging to similar climates.

We conclude that patterns from genomic time series support nonneutral, natural selection–driven evolutionary dynamics, presumably involved in rapid adaptation. Under such rapid adaptation, we may expect that populations that are initially maladapted would decline and then rebound as adaptive genotypes rise in frequency (*30*). By tracking population sizes through annual census (supplementary text S1), eight out of 30 experimental gardens showed average significant signs of population recovery across replicates in the third generation, with a U-shaped trajectory or an increase in population size at the third generation compared with the second, reminiscent of evolutionary rescue [Fig. 2F, figs. S7 to S9, and supplementary text S8 in (*20*)]. Together, the significant allele frequency shifts and the U-shaped population size trajectories support the notion that adaptive evolutionary rescue occurred in some climates.

Rapid evolution follows the pattern of past local adaptation

The strong evidence of rapid adaptation in our experiment is likely attributable to the fact that we drew accessions from natural populations, which presumably were locally adapted to their different native conditions. We next wanted to determine whether our observed rapid adaptation mimics past local adaptation to climatic conditions. Previous studies have found local adaptation in *A. thaliana* (*28*, *29*, *31*–*34*) and many other species (*12*, *13*). Here, we used information on each accession's climate of origin (Fig. 1A) and change in frequency in the experiment (Fig. 3A) to determine whether genotypes from matching climatic origins increased in frequency. We focused on the first-generation sequencing because sampling reproductive adults is a proxy of relative fitness per accession (because $p_{t+1}/p_t = w/\hat{w}$, where w is the fitness of an accession and $\hat{w}$ is the average fitness of the population). We indeed found that accessions that rose in frequency the most in each garden often were originated in climates most similar to those gardens, whereas accessions originated far away failed to propagate in far-away climates, leading to a strong negative correlation of accession success and climate distance to origin across all gardens ($r_\rho = -0.21$, $P < 2 \times 10^{-16}$, $n = 7161$ pairwise garden-to-accession comparisons, averaging replicates within the garden) (Fig. 3A and figs. S32, S34, S35, and S42; see supplementary text S13). To formally quantify climate-driven natural selection, we used a Gaussian local adaptation model (*14*) extended to accession frequency measurements in experimental evolution: $\log(p_{t+1}/p_t) = \log(W_{\max}/\hat{w}) - V_s^{-1}(z_{\text{origin}} - z_{\text{garden}})^2$. Here, $W_{\max}$ denotes the accession-specific maximum fitness at the origin environment, V_s^{-1} denotes the accession-specific strength of natural selection measuring the rate of fitness decay, $\hat{w}$ denotes garden-specific average fitness, z_{garden} denotes the garden environment, and z_{origin} denotes the accession-specific optimal environment (assumed to be the climate of accession origin described by a chosen environmental variable; see details in methods). With this framework, we quantified the strength of climatic local adaptation for each of 19 temperature and precipitation climate variables (BIOCLIM variables calculated from the ERA5-land database; figs. S34 and S40) (*35*). We found evidence of climate adaptation from both temperature and precipitation variables, with the strongest local adaptation signal being annual mean temperature (BIO1) [coefficient of determination (R^2) = 0.337, $P < 2.2 \times 10^{-16}$, $n = 71{,}976$ garden-accession origin transplant combinations; Fig. 3, A and B, and fig. S33).

To understand possible differences between "accession niches," we expanded the Gaussian framework to be accession specific (Fig. 3, B and C, and fig. S39). This revealed a trade-off between maximum fitness and rate of fitness decay across environments (Fig. 3H and fig. S38) (*14*), whereby accessions' maximum fitness negatively correlated with rapid fitness decay when planted in a garden with a different temperature profile ($r_{\rho\ \text{Wmax and Vs-1}} = 0.344$, $P = 8.086 \times 10^{-8}$, $n = 231$ accessions; Fig. 3B and fig. S41). These results are reminiscent of the ecological trade-off observed between specialists and generalists (*29*, *36*). Consequently, we found that "generalist" accessions with wider niches (low V_s^{-1}) are originally from regions of lower habitat suitability at the species distribution range and typically from colder regions [Fig. 3, E and F, and fig. S10; see (*20*)] (*14*), whereas "specialist" accessions with narrower but higher fitness curves appear to come from central-to-warmer native environments ($r_{\text{Vs - temp}} = 0.634$, $P = 2.2 \times 10^{-16}$, $n = 231$ accessions; Fig. 3G) (*37*). For those accessions with narrower niches ($1/V_s > 0.15$), where the local adaptation signal is strongest, we found a notable adaptation lag (*14*, *38*), whereby an accession's realized optimum estimated from the experimental gardens was, on average, colder than the current climate at their geographic origin, on par with the magnitude of ~1.5°C climate change to date (*39*) (estimated optimum − origin temperature = −1.87°C [IQR: −0.796 to −2.84°C]; Fig. 3H).

Because natural selection ultimately operates on phenotypes, we sought to identify the phenotypic basis of rapid adaptation across gardens. Our field observations revealed that spring flowering rapidly synchronized with the expected growth season along a latitudinal temperature gradient within 3 years ($r_{y1} = 0.477$, $P = 0.00671$, $n = 31$ average flowering observations; $r_{y2} = 0.594$, $P = 0.0011$, $n = 27$; $r_{y2} = 0.634$, $P = 0.0026$, $n = 20$; fig. S6). Specifically, flowering periods extended to July in high latitudes and started as early as February in low

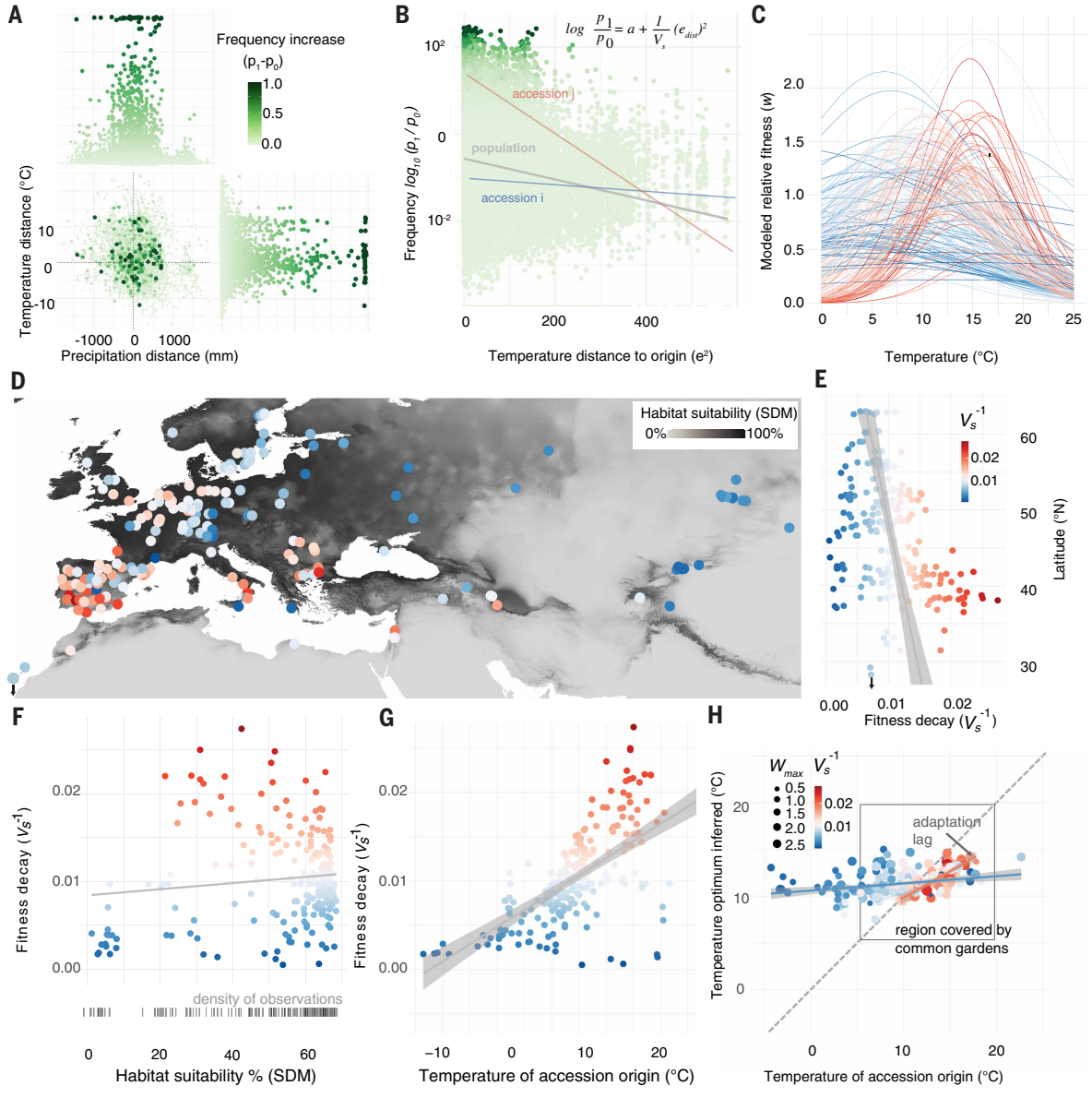

Fig. 3. Rapid evolution follows local adaptation. (**A**) Accession relative frequency change (p_1–p_0) over climatic distance in the first year (n = 75,075 garden-accession origin transplant combinations) showing that planted accessions at sites with annual temperature and precipitation most similar to their home environment typically increase in frequency more than those transplanted to climatically distant environments. (**B**) Transformation of data in (A) to display log(p_1/p_0) and squared temperature distances to fit a model of stabilizing local adaptation. The gray line regression represents the average fitness decline of the GrENE-net accessions with climate distance transplant (i.e., the Gaussian local adaptation parameter V_s^{-1}), whereas accessions *i* and *j* are examples of accession-specific V_s^{-1} slopes. (**C**) Idealized Gaussian local adaptation curves based on fitting (B) equation of V_s and W_{max}. for each of the 231 accessions (see methods). (**D**) Per-accession local adaptation parameter V_s^{-1} visualized in a map of the accessions' geographic collection of origin colored by habitat suitability and (**E**) across a latitudinal gradient of the accession's location origin. The color-coding of accessions represents V_s^{-1}, and the scale is shared for (D) to (H). SDM, species distribution model projecting habitat suitability probability based on range-wide species observations and climate niche (see methods). (**F**) Relationship between the strength of the per-accession local adaptation parameter and habitat suitability of the accessions' locations of origin and (**G**) the accessions' temperatures of origin. (**H**) Annual temperature averages at the accessions' origins against temperatures of gardens weighted by the accessions' frequency, as a proxy of temperature optimum. The gray lines represent regression lines, and the shaded areas indicate their CIs.

latitudes (fig. S4). To extend our phenotypic evolution study to phenotypes that are difficult to measure in the field, we used a curated and imputed database of heritable traits across overlapping *A. thaliana* accessions (*40*) with GrENE-net founder accessions. By correlating ex situ phenotype with the accession's relative frequency change at each garden (supplementary text S15), we found evidence that a number of traits likely diverged across environments (fig. S44). For instance, as proof of concept, using the highly heritable flowering time measured in growth chambers {$h^2_{kinship}$ = 0.93 [95% CI: 0.898–0.975]; (*37*)}, we found that accessions with known late flowering times showed a weak but significant correlation in the coldest locations ($r_{freq\text{ - ft.}}$ = 0.074, P = 4.6 × 10 $^{-6}$, site no. 27 Tartu, Estonia, ~5°C mean annual temperature, n = 225 accessions), whereas in warm locations, the correlation was strong and reversed, with early-flowering accessions becoming more common ($r_{freq\text{ - ft.}}$ = −0.25, P = 1.1 × 10^{-117}, site no. 5 Madrid, Spain, ~14°C mean annual temperature, n = 225). Similarly, strong seed dormancy of accessions (i.e., days of seed dry storage required to reach 50% germination, $h^2_{kinship}$ = 0.987 [95% CI: 0.934–0.998]) correlated

with accession relative frequency increase in warm, low precipitation environments [<100 mm of summer rain (BIO18), Madrid (Spain), and Lesbos (Greece), $r = 0.24$ to 0.25, $P < 10^{-104}$, $n = 225$], where strong dormancy prevents summer germination and increases bet-hedging (*41*–*43*). This follows an expected growth season gradient from late flowering and high autumn germination in high latitudes to early flowering and high seed dormancy in low latitudes (*43*, *44*). Beyond phenology, we found a suite of other traits associated with climatic evolution, such as increased leaf area in cold environments (e.g., <10°C, Warsaw, Poland, $r_{\text{leaf area}} = 0.115$, $P = 2.09 \times 10^{-7}$, $n = 225$) or decreased leaf stomatal density in a summer dry environment (<20 mm of summer precipitation, Lesbos, Greece, $r_{\text{stomata}} = -0.07$, $P = 1.8 \times 10^{-5}$, $n = 225$) (see different phenotypes and environments in figs. S43 and S44 and table S7). Together, these findings support the hypothesis that rapid adaptation trends across local environments are also driven by phenotypic evolutionary divergence.

Mapping the genetic basis of climate adaptation

To map the genetic basis of climate adaptation, we scanned the genome for highly divergent allele frequencies across gardens. We used experimental evolution genome-environment associations (eGEA) to identify SNP frequency changes across experimental gardens associated with environmental selective forces as reflected in BIOCLIM variables (see methods and supplementary text S16 for comparison between classic GEA and eGEA). We used three modeling frameworks: a latent factor mixed model (LFMM) to account for latent dependence of experimental observations and population structure (*45*), a binomial generalized linear model (GLM) to account for variable population sizes, and Kendall-τ ranked correlations (see methods) to detect nonlinear associations in combination with an LD block partition and *P* value pooling with weighted-*Z* analysis (WZA) (figs. S46 to S48) (*46*). After false discovery rate correction, we identified 44 significant blocks associated with multiple climate variables (Fig. 4A and data S9).

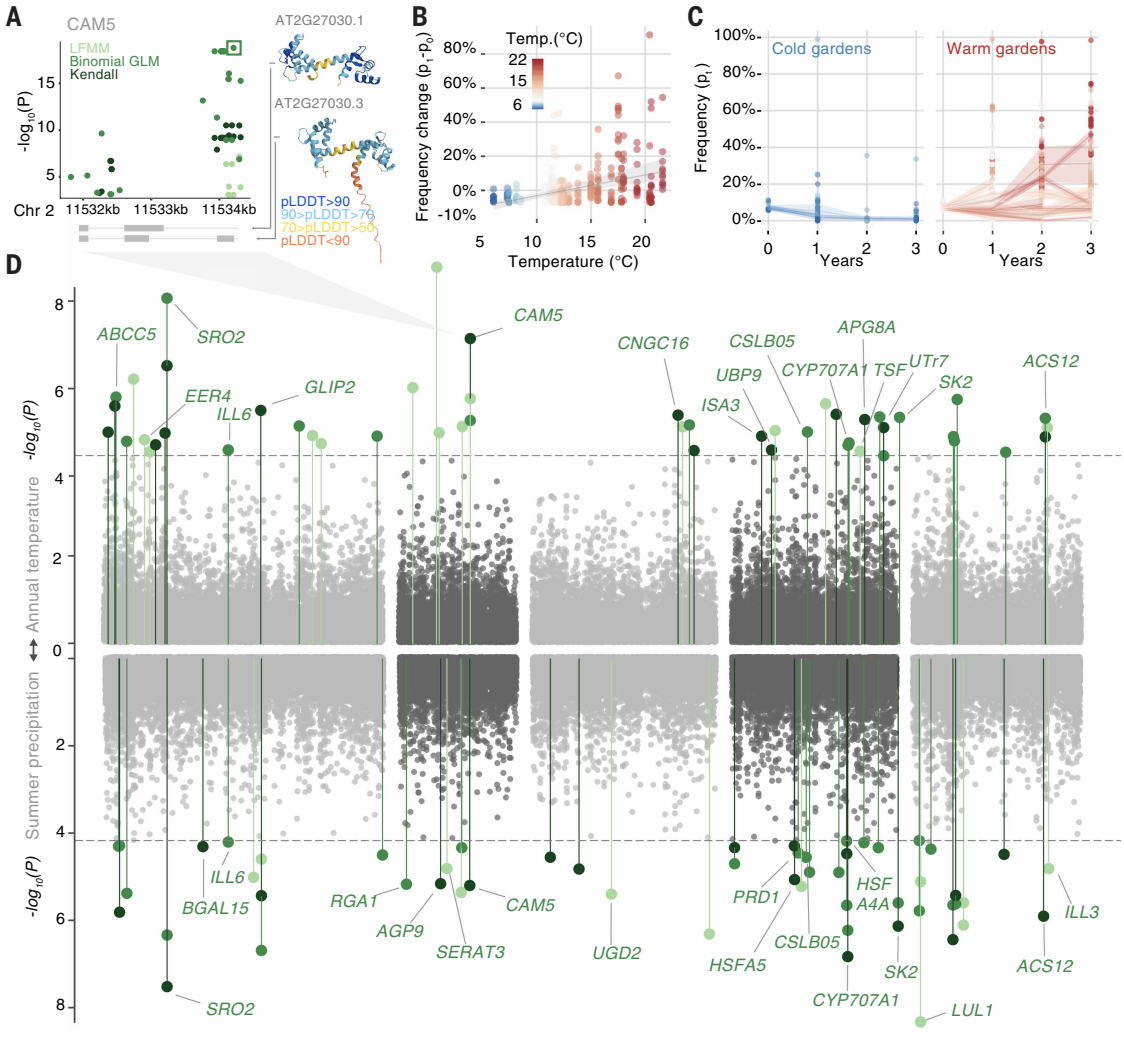

Fig. 4. Rapid adaptation signals along the *A. thaliana* genome. (**A** to **D**) Experimental eGEA of rapid allele frequency trajectories with temperature [(A) to (D)] and precipitation in summer (D) using three statistical approaches: LFMM, quasi-binomial GLM model, and Kendall correlation. (A) is a zoomed-in view of the temperature Manhattan plot with *CAM5* SNP associations, reporting adjusted *P* values using genomic control obtained from the three models for comparison. Final significance is then assessed per LD block with the WZA method (see methods). The protein structures (AlphaFold computed) of two alternative splicing isoforms of the *CAM5* gene are depicted: isoform 1 (AT2G27030.1) and isoform 3 (AT2G27030.3). Gray boxes along the genome (*x* axis) indicate two gene models of the TAIR reference genome, which are present in published transcriptome data (*53*). (B) shows an example of divergent allele frequency trajectories of the *CAM5* top allele (chr4:11533937) across experimental locations along a temperature gradient. Shown in (C) are frequency trajectories of the top *CAM5* allele over years separating experimental gardens in high (>10°C) and low (<10°C) mean annual temperature. (D) is a Manhattan plot of eGEA association of mean annual temperature (up) and summer precipitation (down) that combines results from the three applied statistical approaches with haplotype block *P* value pooling with WZA. Five *A. thaliana* chromosomes are indicated in gray and black.

For an annual plant, both onset of flowering and the timing of germination determine adaptation to seasonal climates, and both vary strongly across the *A. thaliana* range (*43*). It is thus no surprise that blocks identified in our eGEA analyses include loci linked to flowering and dormancy (supplementary text S17 and tables S9 and S10). In our eGEAs, we identified a gene that is well known to be involved in spring flowering—the florigen-encoding gene *TWIN SISTER OF FT* (*TSF*) (*47*–*49*) (LFMM-WZA block significance $P = 3.9 \times 10^{-5}$; LFMM of lead SNP, $P = 3.63 \times 10^{-7}$, Kendall $P = 7.2 \times 10^{-10}$, binomial GLM $P = 3.55 \times 10^{-42}$) (figs. S55 to S57 and supplementary text S17). We also found strong genotype-environment associations for dormancy-related genes such as *CYTOCHROME P450* (*CYP707A1*) (fig. S58 and supplementary text S17), which is a gene that encodes an ABA-catabolic enzyme highly expressed during germination (*50*, *51*). Other eGEA hits with links to stress responses include genes that encode heat shock transcription factors (*HSF4A4*, *HSFA5*) and an aquaporin-like protein (Fig. 4D, figs. S59 and S60, and supplementary text S17).

Furthermore, our eGEA identified blocks harboring genes that have not been previously implicated in climate adaptation. We identified a strong significant association with variation in *CALMODULIN 5* (*CAM5*) in all three eGEA methods (LFMM-WZA $P = 2\times10^{-6}$, Kendall's τ WZA $P = 1 \times 10^{-7}$, binomial GLM WZA $P = 8 \times 10^{-6}$; Fig. 4B) [see supplementary text S17 in (*20*)]. Calmodulins bind stress-triggered calcium to modulate signaling in the context of environmental stress or pathogen responses. *CAM5* expression has been shown to be triggered by high temperature exposure in laboratory conditions (*52*). We found that the top associated SNPs are located in the intron before a third exon that is alternatively spliced (Fig. 4A and figs. S50 and S51). Accessions from warm environments tend to have increased expression of a *CAM5* isoform that includes the alternative third exon downstream of the intron with the top SNP (*53*) ($r = 0.124$, $P = 0.004$, $n = 521$ accessions; fig. S53). In concordance with this prediction, we found that frequencies of alternative alleles in the second *CAM5* intron increase in frequency over time in warm gardens (change rate: +1%/year, $P = 3.58 \times 10^{-15}$, 16 SNPs in 299 populations) and decrease in cold gardens (change rate: −1.6%/year, $P = 1.6 \times 10^{-18}$, 16 SNPs in 56 populations) (Fig. 4, B and C). Taking gardens in both extremes of the temperature gradient, either cold or warm, we estimated selection coefficients on *CAM5* in Cadiz (Spain) to be $s = 57\%$ (95% CI: 49%–66%, $p_{year3} = +46\%$) and in Brixen im Thale (Austria), $s = -47\%$ [95% CI: −56% to −38%, $p_{year2} = 0.2\%$; fig. S52 and see selection estimation in supplementary text S18 in (*20*)]. The magnitude of environment-driven natural selection we inferred on *CAM5* was highly significant but hardly exceptional, with abundant polygenic signals detected along the genome (Fig. 4D). These findings are on par with our observed genome-wide patterns of large selection coefficients and rapid evolutionary responses, akin to those seen in fruit flies or stick insects adapting to seasonal environments (*4*, *54*).

The direction of rapid evolution across climates is predictable

There is an urgent need to predict potential (mal)-adaptation of species to future climates, both for species of conservation focus as well as domesticated species (*55*). We thus asked whether the observed changes in allele frequency ($p_0 \rightarrow p_1$) across experimental evolution gardens could have been predicted from knowledge of the genetic basis of local adaptation of the species. We reasoned that the climatic factors that drive differences in survival in experimental gardens likely also occur in natural populations, so we can use local adaptation signals of natural populations as a predictive signal (*56*). In agreement with this rationale, we found that alleles of warm origins showed upward frequency trajectories [$\Delta p/(1-p)$/°C] in warm experimental gardens and downward trajectories in cold sites ($R^2 = 0.242$, $P < 2.2 \times 10^{-100}$; see Fig. 5A, materials and methods, and fig. S45). Likewise, experimental gardens in similar climates showed concordant changes in allele frequencies [e.g., Madrid versus Barcelona (Spain), $r = 0.657$, $P < 2.2 \times 10^{-100}$; and Cádiz (Spain) versus Lesbos (Greece), $r = 0.733$, $P < 2.2 \times 10^{-100}$, $n = 16{,}757$ LD blocks; Fig. 5B], whereas gardens of contrasting climates showed opposite trajectories [Fig. 5B Konstanz (Germany) versus Madrid (Spain), $r = -0.393$, $P < 2.2 \times 10^{-100}$; and Warsaw (Poland) versus Madrid (Spain), $r = -0.262$, $P = 3.8 \times 10^{-165}$, $n = 16{,}757$ LD blocks] (see systematic analyses of antagonistic pleiotropy in supplementary text S19 and table S11). Such a strong signal is likely driven by a combination of high polygenicity of adaptation, antagonistic pleiotropy, and genome-wide LD (*29*, *57*). Using this signal, we fitted so-called "genomic offset" models that assign the fitness scores of genotypes or populations based on

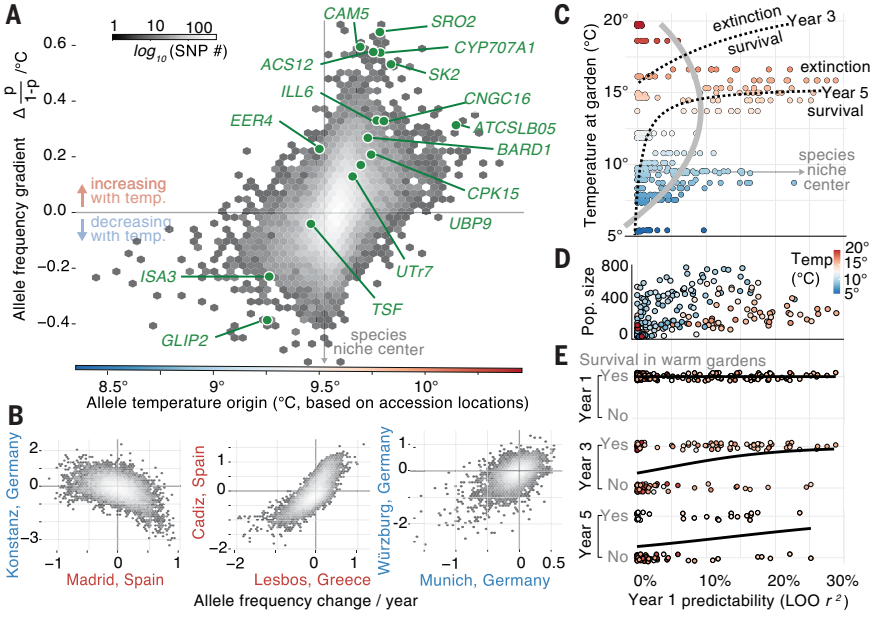

Fig. 5. Predictability of genome-wide evolution and population survival across environments. (**A**) Allele frequency changes with temperature (logistic parameter $\beta = \Delta p/(1-p)$/°C) and its relation to the allele's temperature origin based on the average annual temperature of the *A. thaliana* accessions carrying such alleles. Logistic regression β was calculated per allele and averaged within each LD block ($n = 16{,}656$ LD blocks). Top gene associations (Fig. 4) are highlighted in green. (**B**) Example of allele frequency trajectory over time fitting a logistic regression [$\Delta p/(1-p)$/year], comparing several warm (>10°C, red) and cold (<10°C, blue) experimental gardens (fig. S69). (**C**) Leave-one-out (LOO) predictability of year 1 evolutionary trends [$\log(p_1/p_0)$] per replicate ($n = 325$ populations, $n = 30$ gardens) based on new genomic offset and Gaussian local adaptation across gardens of different temperatures (fig. S69). The gray line indicates the fitted second term polynomial between predictability and temperature. Dotted lines indicate isolines of population survival from fitted logistic regressions in (E). The species niche center represents the average temperature of origin across all founder accessions (9.6°C). (**D**) Relationships between LOO predictability (year 1) and population size over time (summed total number of individuals sampled in years 1 to 3). (**E**) Logistic regressions of LOO predictability of evolutionary trends of population replicates and survival in the first year ($n = 325$ populations), third year ($n = 243$ populations), and fifth year ($n = 139$ populations) (for averages per garden, see fig. S65).

the allelic associations with climate (*58*–*60*) [$GO_{score} = (1/n) \sum (|p_{adapt.,i} - X_{accession,i}|)$; see (*20*)]. Using leave-one-out cross-validation, we aimed to predict evolutionary trajectories for each garden ($p_0 \rightarrow p_1$) using the other gardens as genomic offset training data (Fig. 5C and fig. S63). This showed substantial rank predictive accuracy across all gardens ($r_\rho = 0.263$ [IQR: 0.160–0.368], $P = 5.752 \times 10^{-7}$, $n = 325$ experimental in the first year; r^2 range = 0 to 10.9%) beyond what climate distance alone could predict ($r_\rho = 0.181$ [IQR: 0.020–0.332], $n = 325$; r^2 range = 0 to 10.1%), which is in agreement with previous findings in common gardens of *A. thaliana*, steppe grasses, and poplar tree provenances (*58*, *61*). A similar genomic offset model that additionally incorporated the Gaussian local adaptation model parameters, $V_s^{-1} W_{max}$, has a similar or higher cross-validation predictability {$r_\rho = 0.415$ [IQR: 0.311–0.544], $P < 2.2 \times 10^{-16}$, $n = 325$, r^2 range = 0 to 29.3%; figs. S63 and S64; see (*20*)}.

We ultimately predict early signs of rapid evolution to be informative about long-term population survival in changing climates. So far, evolutionary studies in the wild have typically been limited either by the breadth of climate gradients studied or by the studies' short duration (*62*). To address this gap, we leveraged the geographic span of our experimental evolution plots and the census monitoring for up to 5 years. First, we tested whether predictability of early rapid evolution trends from genomic offset varies across climates. Correlating environmental data with predictability metrics, we found that evolutionary predictability increased with annual temperature (14° to 17°C) but had a significant concave drop at high (>18°C) annual temperatures (regression's quadratic coefficient = −0.001, $P = 2.24 \times 10^{-9}$, $n = 325$ populations in the first year; Figs. 2C and 5C). By contrast, predictability remained lower in cold and wet environments, where mortality was rare and natural selection was presumably low (Fig. 5C). Second, we used logistic regression-based methods to test whether evolutionary predictability was associated with survival or extinction of experimental population replicates. We found climate and evolutionary predictability, as well as their interaction, to be generally significant [Fig. 5E; logistic regression third-year survival: $P_{pred.} = 0.02$, $P_{temp} = 0.02$, interaction $P_{pred. \times temp} = 0.03$ ($n = 243$ populations); fifth-year survival: $P_{pred.} = 0.01$, $P_{temp.} = 0.02$, $P_{pred. \times temp} = 0.02$ ($n = 139$ populations); fig. S6]. The significant interaction indicated that evolutionary predictability correlated with increased survival, especially in the warmest climates: For instance, the likelihood of population survival at ~15°C annual temperature is more than 50% only when initial evolutionary predictability is $r^2 > 15\%$ (see isolines; Fig. 5C). This is reminiscent of eco-evolutionary tipping points that have long been theorized in population genetic literature (*63*), where, in extreme environments, natural selection increases mortality and overpowers the efficiency of evolutionary adaptation, leading to erratic evolutionary trends. Given natural populations of short-lived plants and animals with evidence of evolutionary and demographic responses in subdecadal scales (*4*, *54*, *64*, *65*), our results should be helpful to downscale predictions to conditions with limited genetic diversity or less extreme climate gradients. In the future it will be key to better understand eco-evolutionary tipping points across species that may help us anticipate when species' evolutionary responses may succeed or fail under climate change (*66*).

Materials and methods are available in the supplementary materials.

REFERENCES AND NOTES

1. S. J. Franks, S. Sim, A. E. Weis, Rapid evolution of flowering time by an annual plant in response to a climate fluctuation. *Proc. Natl. Acad. Sci. U.S.A.* **104**, 1278–1282 (2007). doi: 10.1073/pnas.0608379104; pmid: 17220273
2. J. B. Landis *et al.*, Natural selection drives emergent genetic homogeneity in a century-scale experiment with barley. *Science* **385**, eadl0038 (2024). doi: 10.1126/science.adl0038; pmid: 38991084
3. E. D. Enbody *et al.*, Community-wide genome sequencing reveals 30 years of Darwin's finch evolution. *Science* **381**, eadf6218 (2023). doi: 10.1126/science.adf6218; pmid: 37769091
4. A. O. Bergland, E. L. Behrman, K. R. O'Brien, P. S. Schmidt, D. A. Petrov, Genomic evidence of rapid and stable adaptive oscillations over seasonal time scales in Drosophila. *PLOS Genet.* **10**, e1004775 (2014). doi: 10.1371/journal.pgen.1004775; pmid: 25375361
5. P. Nosil *et al.*, Evolution repeats itself in replicate long-term studies in the wild. *Sci. Adv.* **10**, eadl3149 (2024). doi: 10.1126/sciadv.adl3149; pmid: 38787954
6. R. D. H. Barrett *et al.*, Rapid evolution of cold tolerance in stickleback. *Proc. Biol. Sci.* **386**, 233–238 (2011). doi: 10.1098/rspb.2010.0923; pmid: 20685715
7. C. Parmesan, G. Yohe, A globally coherent fingerprint of climate change impacts across natural systems. *Nature* **421**, 37–42 (2003). doi: 10.1038/nature01286; pmid: 12511946
8. M. C. Urban, Climate change extinctions. *Science* **386**, 1123–1128 (2024). doi: 10.1126/science.adp4461; pmid: 39636977
9. M. S. Johnson *et al.*, Phenotypic and molecular evolution across 10,000 generations in laboratory budding yeast populations. *eLife* **10**, e63910 (2021). doi: 10.7554/eLife.63910; pmid: 33464204
10. B. H. Good, M. J. McDonald, J. E. Barrick, R. E. Lenski, M. M. Desai, The dynamics of molecular evolution over 60,000 generations. *Nature* **551**, 45–50 (2017). doi: 10.1038/nature24287; pmid: 29045390
11. J. Clausen, D. D. Keck, W. M. Hiesey, Regional differentiation in plant species. *Am. Nat.* **75**, 231–250 (1941). doi: 10.1086/280955
12. J. Hereford, A quantitative survey of local adaptation and fitness trade-offs. *Am. Nat.* **173**, 579–588 (2009). doi: 10.1086/597611; pmid: 19272016
13. R. Leimu, M. Fischer, A meta-analysis of local adaptation in plants. *PLOS ONE* **3**, e4010 (2008). doi: 10.1371/journal.pone.0004010; pmid: 19104660
14. M. Bontrager *et al.*, Climate warming weakens local adaptationbioRxiv 2020.11.01.364349 [Preprint] (2020); https://doi.org/10.1101/2020.11.01.364349.
15. S. M. Rudman *et al.*, Direct observation of adaptive tracking on ecological time scales in *Drosophila*. *Science* **375**, eabj7484 (2022). doi: 10.1126/science.abj7484; pmid: 35298245
16. M. C. Bitter *et al.*, Continuously fluctuating selection reveals fine granularity of adaptation. *Nature* **634**, 389–396 (2024). doi: 10.1038/s41586-024-07834-x; pmid: 39143223
17. R. D. H. Barrett, D. Schluter, Adaptation from standing genetic variation. *Trends Ecol. Evol.* **23**, 38–44 (2008). doi: 10.1016/j.tree.2007.09.008; pmid: 18006185
18. X. Wu *et al.*, Supplemental datasets for Rapid adaptation and extinction in synchronized outdoor evolution experiments of *Arabidopsis*. Zenodo (2025); https://doi.org/10.5281/zenodo.15360669.
19. K. Bomblies *et al.*, Local-scale patterns of genetic variability, outcrossing, and spatial structure in natural stands of *Arabidopsis thaliana*. *PLOS Genet.* **6**, e1000890–e1000890 (2010). doi: 10.1371/journal.pgen.1000890; pmid: 20361058
20. GrENE-net; see supplementary materials and methods.
21. L. Czech *et al.*, Monitoring rapid evolution of plant populations at scale with Pool-Sequencing. bioRxiv 2022.02.02.477408 [Preprint] (2022); https://doi.org/10.1101/2022.02.02.477408.
22. L. Czech, M. Exposito-Alonso, grenepipe: A flexible, scalable and reproducible pipeline to automate variant calling from sequence reads. *Bioinformatics* **38**, 4809–4811 (2022). doi: 10.1093/bioinformatics/btac600; pmid: 36053180
23. S. Tilk *et al.*, Accurate allele frequencies from ultra-low coverage pool-seq samples in evolve-and-resequence experiments. *G3* **9**, 4159–4168 (2019). doi: 10.1534/g3.119.400755; pmid: 31636085
24. L. Czech, J. P. Spence, M. Expósito-Alonso, grenedalf: Population genetic statistics for the next generation of pool sequencing. *Bioinformatics* **40**, btae508 (2024). doi: 10.1093/bioinformatics/btae508; pmid: 39185959
25. J. K. Kelly, K. A. Hughes, Pervasive linked selection and intermediate-frequency alleles are implicated in an evolve-and-resequencing experiment of *Drosophila simulans*. *Genetics* **211**, 943–961 (2019). doi: 10.1534/genetics.118.301824; pmid: 30593495
26. S. V. Nuzhdin, T. L. Turner, Promises and limitations of hitchhiking mapping. *Curr. Opin. Genet. Dev.* **23**, 694–699 (2013). doi: 10.1016/j.gde.2013.10.002; pmid: 24239053
27. V. Buffalo, G. Coop, Estimating the genome-wide contribution of selection to temporal allele frequency change. *Proc. Natl. Acad. Sci. U.S.A.* **117**, 20672–20680 (2020). doi: 10.1073/pnas.1919039117; pmid: 32817464
28. J. Ågren, D. W. Schemske, Reciprocal transplants demonstrate strong adaptive differentiation of the model organism *Arabidopsis thaliana* in its native range. *New Phytol.* **194**, 1112–1122 (2012). doi: 10.1111/j.1469-8137.2012.04112.x; pmid: 22432639
29. M. Exposito-Alonso, H. A. Burbano, O. Bossdorf, R. Nielsen, D. Weigel; 500 Genomes Field Experiment Team, Natural selection on the *Arabidopsis thaliana* genome in present and future climates. *Nature* **573**, 126–129 (2019). doi: 10.1038/s41586-019-1520-9; pmid: 31462776
30. R. Gomulkiewicz, R. D. Holt, When does evolution by natural selection prevent extinction? *Evolution* **49**, 201–207 (1995). doi: 10.1111/j.1558-5646.1995.tb05971.x; pmid: 28593677
31. A. Fournier-Level *et al.*, A map of local adaptation in *Arabidopsis thaliana*. *Science* **334**, 86–89 (2011). doi: 10.1126/science.1209271; pmid: 21980109
32. A. M. Hancock *et al.*, Adaptation to climate across the arabidopsis thaliana genome. *Science* **334**, 83–86 (2011). doi: 10.1126/science.1209244; pmid: 21980108

33. K. E. Samis, J. R. Stinchcombe, C. J. Murren, Population climatic history predicts phenotypic responses in novel environments for arabidopsis thaliana in North America. *Am. J. Bot.* **106**, 1068–1080 (2019). doi: 10.1002/ajb2.1334; pmid: 31364776
34. L. Leventhal, M. Ruffley, M. Exposito-Alonso, Planting genomes in the wild: Arabidopsis from genetics history to the ecology and evolutionary genomics era. *Annu. Rev. Plant Biol.* **76**, 605–635 (2025). doi: 10.1146/annurev-arplant-071123-095146; pmid: 39971350
35. S. E. Fick, R. J. Hijmans, WorldClim 2: new 1-km spatial resolution climate surfaces for global land areas. *Int. J. Climatol.* **37**, 4302–4315 (2017). doi: 10.1002/joc.5086
36. C. C. Bastias *et al.*, Ecological trade-offs drive phenotypic and genetic differentiation of Arabidopsis thaliana in Europe. *Nat. Commun.* **15**, 5185 (2024). doi: 10.1038/s41467-024-49267-0; pmid: 38890286
37. 1001 Genomes Consortium, 1,135 genomes reveal the global pattern of polymorphism in *Arabidopsis thaliana*. *Cell* **166**, 481–491 (2016). doi: 10.1016/j.cell.2016.05.063; pmid: 27293186
38. A. M. Wilczek, M. D. Cooper, T. M. Korves, J. Schmitt, Lagging adaptation to warming climate in *Arabidopsis thaliana*. *Proc. Natl. Acad. Sci. U.S.A.* **111**, 7906–7913 (2014). doi: 10.1073/pnas.1406314111; pmid: 24843140
39. Intergovernmental Panel on Climate Change (IPCC), "Global warming of 1.5°C," V. Masson-Delmotte *et al.*, Eds. (Cambridge Univ. Press, 2022).
40. M. Ruffley *et al.*, Selection constraints of plant adaptation can be relaxed by gene editing. bioRxiv 2023.10.16.562583 [Preprint] (2024); https://doi.org/10.1101/2023.10.16.562583.
41. I. Kronholm, F. X. Picó, C. Alonso-Blanco, J. Goudet, J. de Meaux, Genetic basis of adaptation in *Arabidopsis thaliana*: Local adaptation at the seed dormancy QTL DOG1. *Evolution* **66**, 2287–2302 (2012). doi: 10.1111/j.1558-5646.2012.01590.x; pmid: 22759302
42. D. S. Vidigal *et al.*, Altitudinal and climatic associations of seed dormancy and flowering traits evidence adaptation of annual life cycle timing in *Arabidopsis thaliana*. *Plant Cell Environ.* **39**, 1737–1748 (2016). doi: 10.1111/pce.12734; pmid: 26991665
43. M. Exposito-Alonso, Seasonal timing adaptation across the geographic range of *Arabidopsis thaliana*. *Proc. Natl. Acad. Sci. U.S.A.* **117**, 9665–9667 (2020). doi: 10.1073/pnas.1921798117; pmid: 32086393
44. M. Debieu *et al.*, Co-variation between seed dormancy, growth rate and flowering time changes with latitude in *Arabidopsis thaliana*. *PLOS ONE* **8**, e61075 (2013). doi: 10.1371/journal.pone.0061075; pmid: 23717385
45. K. Caye, B. Jumentier, J. Lepeule, O. François, LFMM 2: Fast and accurate inference of gene-environment associations in genome-wide studies. *Mol. Biol. Evol.* **36**, 852–860 (2019). doi: 10.1093/molbev/msz008; pmid: 30657943
46. T. R. Booker, S. Yeaman, J. R. Whiting, M. C. Whitlock, The WZA: A window-based method for characterizing genotype-environment associations. *Mol. Ecol. Resour.* **24**, e13768 (2024). doi: 10.1111/1755-0998.13768; pmid: 36785926
47. A. Yamaguchi, Y. Kobayashi, K. Goto, M. Abe, T. Araki, *TWIN SISTER OF FT* (*TSF*) acts as a floral pathway integrator redundantly with FT. *Plant Cell Physiol.* **46**, 1175–1189 (2005). doi: 10.1093/pcp/pci151; pmid: 15951566
48. S. Jang, S. Torti, G. Coupland, Genetic and spatial interactions between *FT*, *TSF* and *SVP* during the early stages of floral induction in *Arabidopsis*. *Plant J.* **60**, 614–625 (2009). doi: 10.1111/j.1365-313X.2009.03986.x; pmid: 19656342
49. W. Kim, T. I. Park, S. J. Yoo, A. R. Jun, J. H. Ahn, Generation and analysis of a complete mutant set for the *Arabidopsis FT/TFL1* family shows specific effects on thermo-sensitive flowering regulation. *J. Exp. Bot.* **64**, 1715–1729 (2013). doi: 10.1093/jxb/ert036; pmid: 23404901
50. M. Okamoto *et al.*, CYP707A1 and CYP707A2, which encode abscisic acid 8′-hydroxylases, are indispensable for proper control of seed dormancy and germination in *Arabidopsis*. *Plant Physiol.* **141**, 97–107 (2006). doi: 10.1104/pp.106.079475; pmid: 16543410
51. H. He *et al.*, Interaction between parental environment and genotype affects plant and seed performance in *Arabidopsis*. *J. Exp. Bot.* **65**, 6603–6615 (2014). doi: 10.1093/jxb/eru378; pmid: 25240065
52. N. A. Al-Quraan, R. D. Locy, N. K. Singh, Expression of calmodulin genes in wild type and calmodulin mutants of *Arabidopsis thaliana* under heat stress. *Plant Physiol. Biochem.* **48**, 697–702 (2010). doi: 10.1016/j.plaphy.2010.04.011; pmid: 20554213
53. T. Kawakatsu *et al.*, Epigenomic diversity in a global collection of *Arabidopsis thaliana* accessions. *Cell* **166**, 492–505 (2016). doi: 10.1016/j.cell.2016.06.044; pmid: 27419873
54. P. Nosil *et al.*, Natural selection and the predictability of evolution in *Timema* stick insects. *Science* **359**, 765–770 (2018). doi: 10.1126/science.aap9125; pmid: 29449486
55. T. Capblancq, M. C. Fitzpatrick, R. A. Bay, M. Exposito-Alonso, S. R. Keller, Genomic prediction of (mal)adaptation across current and future climatic landscapes. *Annu. Rev. Ecol. Evol. Syst.* **51**, 245–269 (2020). doi: 10.1146/annurev-ecolsys-020720-042553
56. K. E. Lotterhos, The paradox of adaptive trait clines with nonclinal patterns in the underlying genes. *Proc. Natl. Acad. Sci. U.S.A.* **120**, e2220313120 (2023). doi: 10.1073/pnas.2220313120; pmid: 36917658
57. C. G. Oakley, D. W. Schemske, J. K. McKay, J. Ågren, Ecological genetics of local adaptation in *Arabidopsis*: An 8-year field experiment. *Mol. Ecol.* **32**, 4570–4583 (2023). doi: 10.1111/mec.17045; pmid: 37317048
58. M. C. Fitzpatrick, V. E. Chhatre, R. Y. Soolanayakanahally, S. R. Keller, Experimental support for genomic prediction of climate maladaptation using the machine learning approach Gradient Forests. *Mol. Ecol. Resour.* **21**, 2749–2765 (2021). doi: 10.1111/1755-0998.13374; pmid: 33683822
59. C. R. Mahony *et al.*, Evaluating genomic data for management of local adaptation in a changing climate: A lodgepole pine case study. *Evol. Appl.* **13**, 116–131 (2019). doi: 10.1111/eva.12871; pmid: 31892947
60. C. Rellstab, B. Dauphin, M. Exposito-Alonso, Prospects and limitations of genomic offset in conservation management. *Evol. Appl.* **14**, 1202–1212 (2021). doi: 10.1111/eva.13205; pmid: 34025760
61. J. T. Lovell *et al.*, Genomic mechanisms of climate adaptation in polyploid bioenergy switchgrass. *Nature* **590**, 438–444 (2021). doi: 10.1038/s41586-020-03127-1; pmid: 33505029
62. J. T. Stroud, W. C. Ratcliff, Long-term studies provide unique insights into evolution. *Nature* **639**, 589–601 (2025). doi: 10.1038/s41586-025-08597-9; pmid: 40108318
63. J. Polechová, N. H. Barton, Limits to adaptation along environmental gradients. *Proc. Natl. Acad. Sci. U.S.A.* **112**, 6401–6406 (2015). doi: 10.1073/pnas.1421515112; pmid: 25941385
64. D. N. Anstett *et al.*, Evolutionary rescue during extreme drought. bioRxiv 2024.10.24.619808 [Preprint] (2024); https://doi.org/10.1101/2024.10.24.619808.
65. S. J. Franks, N. C. Kane, N. B. O'Hara, S. Tittes, J. S. Rest, Rapid genome-wide evolution in Brassica rapa populations following drought revealed by sequencing of ancestral and descendant gene pools. *Mol. Ecol.* **25**, 3622–3631 (2016). doi: 10.1111/mec.13615; pmid: 27072809
66. A. A. Hoffmann, C. M. Sgrò, Climate change and evolutionary adaptation. *Nature* **470**, 479–485 (2011). doi: 10.1038/nature09670; pmid: 21350480

ACKNOWLEDGMENTS

We thank D. Petrov, S. Rudman, M. Schumer, and B. Good for feedback from and discussions on genomic and rapid adaptation; A. Holehouse for discussions of intrinsically disordered domains; and M. Nordborg for discussions on initial project design. We thank J. Kelly for his help with running LRT-1 analysis and T. Booker for discussions of WZA code. We thank the members of the MOILAB for feedback on the research and manuscript. We are grateful to all colleagues in the *Arabidopsis* field that have maintained a vibrant seed collection and shared resources. The GrENE-net consortium acknowledges D. Zerning and L. Westphal for garden support in MPI Potsdam-Golm and thanks colleagues D. Salt, P. Kover, and A. Hancock, who showed support in this collaborative network in its early stages of development. **Funding:** M.E.-A. is supported by the Office of the Director of the National Institutes of Health's Early Investigator Award (1DP5OD029506-01); the US Department of Energy, Office of Biological and Environmental Research (DE-SC0021286); the US National Science Foundation's DBI Biology Integration Institute WALII (Water and Life Interface Institute, 2213983); the Carnegie Institution for Science; the Howard Hughes Medical Institute; the Innovative Genomics Institute; and the University of California, Berkeley. Computational analyses were done on the High-Performance Computing clusters of the Carnegie Institution for Science and High Performance Computing cluster of the University of California, Berkeley. Part of genome sequencing was performed at the QB3 Genomics facilities at the University of California, Berkeley (RRID:SCR_022170). GrENE-net consortium funding is as follows: C.A.-B.'s laboratory was funded by grant PID2022-136893NB-I00 from the MCIN/MCIU/AEI/10.13039/501100011033 and FEDER (EU). F.X.P. was funded by grant PID2023-147962NB-I00 from the MCIN/MCIU/AEI/10.13039/501100011033 and FEDER (EU). M.P. was supported by the Estonian Research Council (PRG3127) and the Estonian Ministry of Education and Research (Centre of Excellence AgroCropFuture, TK200), C.L.-R. was supported by Juan de la Cierva Formación postdoctoral fellowship FJCI-2015-24712 and by Juan de la Cierva Incorporación postdoctoral fellowship (IJC2019-041342-I). A.G.-F., C.L.-R., J.M.I., and J.M.-L. have support from grant PID2021-127841OA-I00/AEI/10.13039/501100011033/FEDER, UE. M.B. and M.A. were funded by a grant from the Organismo Autónomo de Parques Nacionales globalHybrids 2415/2017. A.G.-M. and M.A. were funded by grant PID2019-111294GB-I00/SRA/10.13039/501100011033. J.d.M. was funded by Deutsche Forschungsgemeinschaft (DFG, German Research Foundation) under the Research Consortium TRR341 "Plant Ecological Genetics" as well as under Germany's Excellence Strategy–EXC-2048/1–project ID390686111. C.D. and M.Q. were supported by the Deutsche Forschungsgemeinschaft (DFG, 514901783) through the Collaborative Research Centre 1664 "Plant Proteoform Diversity—SNP2Prot." **Author contributions:** M.E.-A., J.F.S., and F.V. conceptualized the experiment and co-led the coordination of GrENE-net. M.E.-A. led and coordinated this first GrENE-net paper, data production, and release, including sample curation, genomic sequencing, and data analyses. O.B., R.C. and D.W. provided initial support and resources for starting this initiative at the University of Tübingen and Max Planck Institute for Biology Tübingen. All GrENE-net participants contributed to experimental design and running the experiment. M.E.-A. and J.F.S. coordinated sample handling. Sample processing and genomic sequencing was conducted in M.E.-A.'s laboratory. Y.P. performed DNA sample processing and sequencing with advice from P.L. T.B. and M.L. performed experimental data curations and climate data retrieval. L.C., X.W., T.B., M.L., and M.E.-A. conducted software development. X.W., T.B., M.L., L.C., R.E., and M.E.-A. performed genomic analyses. B.Q.-C. and K.D. performed the dispersal experiment and data analyses. Data interpretation was conducted by all authors. The manuscript was drafted by M.E.-A., X.W., and T.B. and edited, commented on, discussed, and improved by all authors. GrENE-net consortium authors are listed in alphabetical order in the byline. **Competing interests:** D.W. holds equity in Computomics, which advises plant breeders. D.W. also consulted for KWS SE, a globally active plant breeder and seed producer. All other authors declare no competing financial interests. The funders had no role in study design, data collection and analysis, the decision to publish, or preparation of the manuscript. **Data, code, and materials availability:** All datasets and links to repositories are available in www.GrENE-net.org/data. Tables S1 to S18 are

available as supplementary materials and also in Zenodo (*18*). Supplementary datasets and processed intermediate genomic files are available in Zenodo (*18*). Cleaning scripts, sample records, meta-data, and plant census are available at https://github.com/moiexpositoalonsolab/grene and in Zenodo (*113*). Sequencing Illumina reads for GrENE-net experimental evolution plots are deposited at the National Center for Biotechnology Information (NCBI) with accession no. PRJNA1256468 (https://www.ncbi.nlm.nih.gov/sra/PRJNA1256468). Founder genomes are available at https://1001genomes.org/data/GMI-MPI/releases/v3.1. Scripts to reproduce analyses and figures are available at: https://github.com/moiexpositoalonsolab/grenephase1-paper and in Zenodo (*106*). Software to analyze pool sequencing data are available at https://github.com/moiexpositoalonsolab/grenepipe and in (*22*), at https://github.com/lczech/grenedalf and in (*24*), and at https://github.com/moiexpositoalonsolab/hapfire and in Zenodo (*108*). The 1001G seed collection can be obtained from the *Arabidopsis* Biological Resource Center (ABRC) under accession no. CS78942.

SUPPLEMENTARY MATERIALS

science.org/doi/10.1126/science.adz0777
Materials and Methods; Supplementary Text; Figs. S1 to S67; Tables S1 to S18; References (*67*–*142*); MDAR Reproducibility Checklist

Submitted 4 June 2025; accepted 12 December 2025

10.1126/science.adz0777

Rapid adaptation and extinction in synchronized outdoor evolution experiments of *Arabidopsis*

Xing Wu, Tatiana Bellagio, Yunru Peng, Lucas Czech, Meixi Lin, Patricia Lang, Ruth Epstein, Mohamed Abdelaziz, Jake Alexander, Carlos Alonso-Blanco, Heidi Lie Andersen, Modesto Berbel, Joy Bergelson, Oliver Bossdorf, Liana Burghardt, Mireille Caton-Darby, Robert Colautti, Carolin Delker, Panayiotis G. Dimitrakopoulos, Kathleen Donohue, Walter Durka, Gema Escribano-Avila, Steven J. Franks, Felix B. Fritschi, Alexandros Galanidis, Alfredo Garcia-Fernández, Ana García-Muñoz, Elena Hamann, Allison Hutt, José M. Iriondo, Thomas E. Juenger, Stephen R. Keller, Karin Koehl, Arthur Korte, Pamela Korte, Alexander Kutschera, Carlos Lara-Romero, Laura Leventhal, Daniel Maag, Arnald Marcer, Martí March-Salas, Juliette de Meaux, Belén Méndez-Vigo, Javier Morente-López, Timothy C. Morton, Zuzana Münzbergova, Anne Muola, Hanna Akiko Nomoto, Meelis Pärtel, F. Xavier Picó, Brandie Quarles-Chidyagwai, Marcel Quint, Niklas Reichelt, Agnieszka Rudak, Johanna Schmitt, Gregor Schmitz, Merav Seifan, Basten L. Snoek, Remco Stam, Marc Stift, John R. Stinchcombe, Mark A. Taylor, Peter Tiffin, Irène Till-Bottraud, Anna Traveset, Jean-Gabriel Valay, Martijn Van Zanten, Vigdis Vandvik, Cyrille Violle, Detlef Weigel, Maciej Wódkiewicz, François Vasseur, J. F. Scheepens, and Moises Exposito-Alonso

Science **391** (6792), eadz0777. DOI: 10.1126/science.adz0777

Editor's summary

For organisms with generation times longer than those in yeast or bacteria, testing the repeatability of evolution in differing environmental conditions takes a great deal of time and resources. Wu *et al*. enlisted the help of citizen scientists in Europe, the Levant, and the US to grow 12 replicates of the same array of 231 *Arabidopsis thaliana* accessions to see how the populations evolved over 5 years. Over the 30 locations where the plants grew successfully, the authors found that frequency shifts largely replicated within gardens, and that these shifts tended to be similar between locations with similar environments. This large undertaking gives insight into how these plants may evolve in response to future changing pressures such as climate change. —Corinne Simonti